Steel Built-up Girders with Trapezoidally Corrugated Webs

MOHAMED ELGAALY and ANAND SESHADRI

INTRODUCTION

The availability of high strength steels requires innovative designs, such as the use of corrugated webs, for efficient use of these steels. Economical design of steel girders normally requires thin webs; the conventional welding of stiffeners to allow the use of thin webs has two disadvantages. The first is high fabrication cost, and the second is a possible reduced life due to fatigue cracking which may initiate at the stiffeners weld. The use of corrugated plates in lieu of flat stiffened plates in the web of a girder can eliminate both disadvantages. With the advances in welding technology, automatic welding of corrugated webs can benefit from the joint tracking technology,[1] and the web needs to be welded to the flanges only from one side. As a result, girders with corrugated webs can be very economical when compared with conventionally stiffened girders. Furthermore, the use of corrugated webs will increase the lateral stiffness of the girder, thus minimize lateral-torsional buckling bracing requirements, particularly during construction, and the use of corrugated webs in composite construction will minimize cracking of the slab.

Studies on the behavior of beams with corrugated webs subjected to shear have been conducted in the United States: Peterson,[2] Rothwell,[3] Sherman and Fisher,[4] Libove,[5,6] Easley,[7] Wu and Libove,[8] and Hussain and Libove.[9] Studies were conducted in Britain by Harrison,[10] in Hungary by Korashy and Varga,[11] in Sweden by Bergfelt and Aravena,[12] and in Germany by Lindner[13,14] and by Scheer and Einsiedler.[15]

Beams with corrugated webs have been manufactured in Sweden, Germany, and Japan,[16] and used in buildings in the United States, Europe, and Japan, and in Bridges in France.[17,18] A summary of the research and Development in beams and girders with corrugated webs was reported by Elgaaly and Dagher.[19] Research work on the behavior of steel built-up girders with corrugated webs under different loading conditions was conducted by Elgaaly at the University of Maine and at Drexel University. Results from this research work were published,[20,21,22] and this paper address the design of built-up steel girders made of trapezoidally corrugated webs.

Mohamed Elgaaly is professor, department of civil and architectural engineering, Drexel University, Philadelphia, PA.

Anand Seshadri was formerly a graduate student at Drexel University.

SHEAR CAPACITY BASED ON LOCAL BUCKLING

The mode of failure of a steel built-up girder with corrugated web subjected to shear is local and/or global buckling of the web, as shown in Figure 1. In the local buckling mode, the corrugated web acts as a series of flat plate sub-panels, made of the corrugation folds, that mutually support each other along their vertical edges and are supported by the flanges at their horizontal edges. These flat plate sub-panels (folds) are subjected to shear; and the elastic buckling stress is given by,

$$\tau_{cre} = k_s[\pi^2 E / 12(1 - \mu^2)(w/t)^2] \quad (1)$$

where

k_s = Buckling coefficient which is function of the panel aspect ratio (h/w) and the boundary support conditions
h = The web depth
t = The web thickness
w = The fold width – the horizontal or the inclined, whichever is bigger

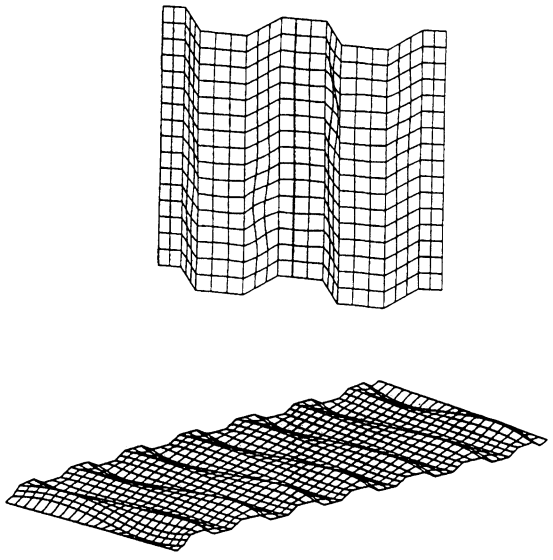

Fig. 1. Local and global buckling of the web due to shear.

E = Young's Modulus of Elasticity
μ = Poisson's ratio

The buckling coefficient k_s is given by

$$k_s = 5.34 + 2.31(w/h) - 3.44(w/h)^2 + 8.39(w/h)^3$$

for the longer edges simply-supported and the shorter edges clamped, and

$$k_s = 8.98 + 5.6(w/h)^2$$

in the case where all edges are clamped.

In case $\tau_{cre} > 0.8\tau_y$, inelastic buckling will occur and the inelastic buckling stress τ_{cri} can be calculated by,

$$\tau_{cri} = (0.8 \times \tau_{cre} \times \tau_y)^{0.5} \leq \tau_y \quad (2)$$

The local buckling stresses were calculated for test specimens[23] with coarse corrugations made of three different profiles, 2-in., $2\frac{1}{16}$-in., and 1-in. deep, as shown in Figure 2. The web panels of the test specimens have four different aspect ratios (panel width-to-depth ratio equals 0.5, 1.0, 1.5, and 2.0) and three different depths of 12-in., 18-in., and 24-in. In the calculations, the corrugation folds were assumed to have two boundary conditions; simply supported along the longer edges and clamped along the shorter edges τ_{ssf}, and clamped along all four edges τ_{fx}. The calculated stresses are given in Table 1 and are compared with the corresponding stresses

Dimensions of Test Specimens

Identification	*a* (in.)	*h* (in.)	Thickness A (in.)	Thickness B (in.)	Aspect Ratio (*a* / *h*)	Configuration
V121216A or B	12	12	0.0251	0.0301	1:1	UF1X
V121221A or B	12	12	0.0248	0.0309	1:1	UFX-36
V121232A or B	12	12	0.0252	0.0307	1:1	UF2X
V121809A or B	18	12	0.0278	0.0249	1.5:1	UFS
V121832A or B	18	12	0.0252	0.0362	1.5:1	UF2X
V122409A or B	24	12	0.0281	0.0261	2:1	UFS
V122421A or B	24	12	0.0266	0.0308	2:1	UFX-36
V122432A or B	24	12	0.0252	0.0306	2:1	UF2X
V181209A or B	12	18	0.0220	0.0240	1:1.5	UFS
V181216A or B	12	18	0.0240	0.0299	1:1.5	UF1X
V181221A or B	12	18	0.0240	0.0300	1:1.5	UFX-36
V181232A or B	12	18	0.0235	0.0295	1:1.5	UF2X
V181809A or B	18	18	0.0240	0.0245	1:1	UFS
V181816A or B	18	18	0.0250	0.0290	1:1	UF1X
V181821A or B	18	18	0.0250	0.0290	1:1	UFX-36
V181832A or B	18	18	0.0240	0.0295	1:1	UF2X
V241209A or B	12	24	0.0245	0.0250	1:2	UFS
V241216A or B	12	24	0.0250	0.0310	1:2	UF1X
V241221A or B	12	24	0.0240	0.0300	1:2	UFX-36
V241232A or B	12	24	0.0245	0.0300	1:2	UF2X

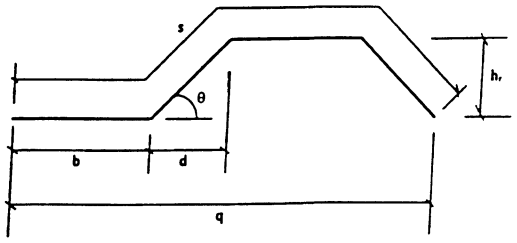

Corrugation Configurations

Profile Type	*b* (in.)	*d* (in.)	h_r (in.)	θ (degrees)	*s* (in.)	*q* (in.)
UFS	0.78	0.47	$\frac{9}{16}$	50.0	3.00	2.50
UF1X	1.50	1.00	$\frac{16}{16}$	45.0	5.83	5.00
UFX-36	1.65	0.92	$\frac{21}{16}$	55.0	6.50	5.14
UF2X	1.96	1.04	$\frac{32}{16}$	62.5	8.43	6.00

Fig. 2. Dimensions of shear test specimens and corrugation profiles.

Table 1.
Shear Stresses from Tests τ_e, F. E. Analysis τ_f, and Based on Local Buckling

Specimen	τ_f, ksi	τ_e, ksi	τ_e/τ_f	τ_y, ksi	τ_{ssf}, ksi	τ_f/τ_{ssf}	τ_{fx}, ksi	τ_f/τ_{fx}	τ_f/τ_{av}
V121216A	44.92	37.35	0.83	56.58	41.02	1.10	54.87	0.82	0.94
V121216B	52.71	54.54	1.04	55.71	51.27	1.03	65.29		0.99
V121221A	39.95	34.95	0.88	55.71	33.23	1.20	48.96	0.82	0.97
V121221B	52.72	43.96	0.83	55.71	47.95	1.10	61.00	0.95	1.02
V121232A	31.68	30.59	0.97	55.71	18.76	1.69	30.16	1.05	1.30
V121232B	43.97	37.32	0.85	53.69	27.84	1.58	43.85	1.00	1.23
V121832A	24.11	25.63	1.06	58.89	18.76	1.29	30.16	0.80	0.99
V121832B	43.26	27.62	0.64	47.05	38.17	1.13	48.40	0.92	1.02
V122421A	35.18	30.48	0.87	51.96	38.23	0.92	50.71	0.69	0.79
V122421B	50.49	37.23	0.74	53.41	46.8	1.08	59.53	0.95	1.01
V122432A	27.31	23.15	0.85	59.76	18.76	1.46	30.16	0.91	1.12
V122432B	33.01	29.96	0.91	53.12	27.66	1.19	43.47	0.76	0.93
V181216A	40.12	48.61	1.21	51.78	36.98	1.09	50.06	0.80	0.92
V181216B	55.46	49.91	0.90	56.82	51.07	1.09	65.33	0.98	1.03
V181221A	34.79	32.18	0.93	48.39	30.65	1.14	44.01	0.79	0.93
V181221B	47.57	40.74	0.86	50.74	44.09	1.08	56.33	0.94	1.00
V181232A	23.57	27.42	1.16	46.19	15.98	1.48	25.92	0.91	1.13
V181232B	33.33	33.90	1.02	50.44	25.18	1.32	40.60	0.82	1.01
V181816A	41.69	37.33	0.90	49.53	39.88	1.05	51.00	0.84	0.93
V181816B	51.44	41.42	0.81	51.40	47.12	1.09	60.26	1.00	1.04
V181821A	35.13	28.22	0.80	46.19	33.26	1.06	44.79	0.78	0.90
V181821B	45.08	40.23	0.89	49.91	42.27	1.07	54.01	0.90	0.98
V181832A	27.69	27.55	1.00	57.74	16.67	1.66	27.03	1.02	1.27
V181832B	31.68	33.30	1.05	48.57	25.18	1.26	39.84	0.80	0.98
V241216A	40.83	28.32	0.69	49.53	39.73	1.03	50.95	0.82	0.92
V241216B	49.36	40.30	0.82	49.23	49.11	1.01	62.99	1.00	1.00
V241221A	36.09	30.16	0.84	51.05	30.41	1.19	45.15	0.80	0.96
V241221B	46.69	39.57	0.85	53.48	45.08	1.04	57.77	0.87	0.95
V241232A	26.87	26.41	0.98	56.38	17.19	1.56	28.05	0.96	1.19
V241232B	33.53	31.68	0.95	48.93	25.78	1.30	40.58	0.83	1.01

from finite element analysis[24] τ_f and the test results τ_e. The non-linear finite element analysis consider both geometric and material non-linearities, and the computer program ABAQUS was used. An average local buckling stress was calculated for all the specimens, where

$$\tau_{av} = 0.5[\tau_{ssf} + \tau_{fx}] \tag{3}$$

As can be noted the average local buckling stresses τ_{av} agree reasonably well with the corresponding stresses from the finite element analysis τ_f; the average ratio τ_f/τ_{av} was calculated to be 1.015 for all the values given in Table 1. The experimental results are, in general, lower than the finite element analysis results due to the presence of unavoidable initial geometric imperfections in the webs of the test specimens.

SHEAR CAPACITY BASED ON GLOBAL BUCKLING

In the case of dense corrugations global buckling controls. The buckling stress can be calculated for the entire corrugated web panel, using orthotropic-plate buckling theory. The global elastic buckling stress τ_{cre}, can be calculated from,

$$\tau_{cre} = k_s[(D_x)^{0.25}(D_y)^{0.75}]/th^2 \tag{4}$$

where

$D_x = (q/s)Et^3/12$
$D_y = EI_y/q$
$I_y = 2bt(h_r/2)^2 + \{t(h_r)^3/6\sin\theta\}$
k_s = Buckling coefficient, equals 31.6 for simply supported boundaries and 59.2 for clamped boundaries
t = corrugated plate thickness
b, h_r, q, s, and θ are as shown in Figure 2

Again, when $\tau_{cre} > 0.8\tau_y$, inelastic buckling will occur and the inelastic buckling stress τ_{cri} can be calculated using Equation 2.

The global buckling stresses for test specimens[23] made of a dense corrugation, 5/16-in. deep as shown in Figure 2, were calculated using the buckling formula for the orthotropic plate and a buckling coefficient, k_s equals 59. The aspect ratio and depth of the web panels tested are similar to those previously

Table 2.
Shear Stresses from Tests τ_e, F. E. Analysis τ_f, and Based on Global Buckling

Specimen	τ_f, ksi	τ_e, ksi	τ_e/τ_f	τ_y, ksi	τ_{cre}, ksi	τ_{cri}, ksi	τ_{cr}, ksi	τ_f/τ_{cr}
V121809A	48.59	42.57	0.88	47.92	129.7	70.52	47.92	1.01
V121809B	54.72	41.50	0.76	56.00	122.8	74.16	56.00	0.98
V122409A	44.34	38.55	0.87	49.07	130.4	71.55	49.07	0.90
V122409B	56.87	41.51	0.73	51.96	125.7	72.28	51.96	1.10
V181209A	57.93	45.96	0.79	57.74	51.29	48.67	48.67	1.19
V181209B	56.78	46.20	0.81	49.58	53.58	46.10	46.10	1.23
V181809A	51.46	42.82	0.83	51.77	53.58	47.11	47.11	1.09
V181809B	45.87	39.57	0.86	46.79	54.12	45.01	45.01	1.02
V241209A	32.48	27.06	0.83	50.74	30.46	—	30.46	1.07
V241209B	33.28	29.72	0.89	51.96	30.74	—	30.74	1.08

Note: τ_{cr} = Minimum (τ_y, τ_{cre}, τ_{cri})

given for the specimens with coarse corrugation profiles. The results are given in Table 2 together with the experimental results[23] and the results from finite element analysis.[24] The average value of the ratio between the Finite Element analysis results and those obtained from the orthotropic plate theory τ_f/τ_{cr} is 1.067. Again, the experimental results are lower than the results from the finite element analysis due to the presence of initial geometric imperfections in the webs of the test specimens.

For practical application, it is recommended that the local and global buckling stresses be calculated and the smaller value controls. Furthermore when the buckling stress is bigger than 80 percent of the yield stress the inelastic buckling stress can be calculated using the semi-empirical formula given by Equation 2.

BENDING CAPACITY

The contribution of the web to the ultimate moment capacity of a beam with corrugated web is negligible, and the ultimate moment capacity will be based on the flange yield stress. The stresses in the web due to bending are equal to zero except very close to the flanges where the web is restrained. This conclusion was reached based on experimental[23] and analytical[24] studies. In the experimental studies all the specimens tested[23] failed due to flange yielding followed by vertical buckling of the compression flange into the web, as shown in Figure 3. In the analytical studies[24] the corrugation profile, the ratio between the web and flange yield stresses, the ratio between the web and flange thickness, and the panel aspect ratio were among the parameters considered.

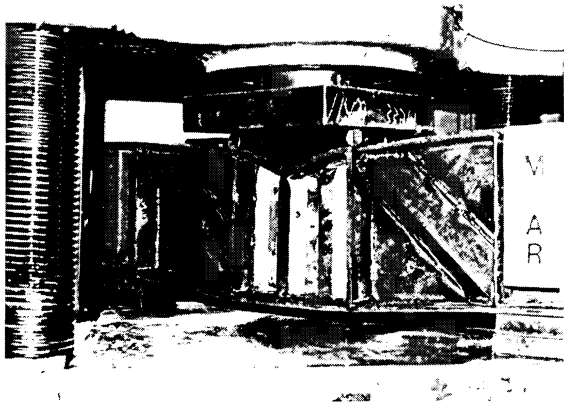

Fig. 3. Failure due to bending.

Since the shear is carried entirely by the web and is controlled by buckling and the moment is carried entirely by the flanges, there is no interaction between bending and shear. Based on limited analytical studies[24] using finite elements, the bracing requirements of the compression flange in beams and girders with corrugated webs are less demanding compared to conventional beams and girders with flat webs. Lateral-torsional buckling of beams and girders with corrugated webs has been investigated by Lindner.[13]

CAPACITY FOR COMPRESSIVE EDGE LOADING

Girders with corrugated webs can be subjected to local compressive loads; examples of such loads include wheel loads and loads from beams resting on the top flange of the girder. Bearing stiffeners at the location of the loads can be provided, however, they are costly and are not feasible in the case of moving loads; hence, there is a need to find the capacity of corrugated webs under partial compressive edge loads. The width of the load can vary between zero (line load) and a load with a width equals to the width of several folds of the corrugation. The load can be over a horizontal or an inclined fold, it can be over the fold line between a horizontal and inclined folds, or it can be over several folds.

Five tests were conducted in addition to extensive numerical analysis, using finite elements, and analytical studies.[24] In addition to the writers' five tests, six tests were conducted in Sweden.[25] In all these analytical and experimental studies, two distinct modes of failure were observed. The first, mode I, includes a collapse mechanism in the loaded flange and

Table 3-1.
Load Over a Parallel Fold, Profile I

Girder	t_f (in.)	t_w (in.)	F_{yf} (ksi)	F_{yw} (ksi)	N/b_h	P_f (kips)	a (in.)	P_{fl} (kips)	P_w (kips)	P_u (kips)	P_f / P_u
Girder 1	0.50	0.1046	36.0	36.0	1.00	34.59	4.53*	20.73	11.18	31.91	1.08
Girder 1A	0.50	0.1046	36.0	36.0	1.00	35.30	4.53*	20.73	11.18	31.91	1.11
Girder 2	0.50	0.1046	65.0	36.0	1.00	45.53	5.59	31.29	11.18	42.47	1.07
Girder 3	0.50	0.1046	100.0	36.0	1.00	47.03	6.59	38.81	11.18	49.99	0.94
Girder 4	0.50	0.1046	36.0	65.0	1.00	36.96	3.74*	20.73	15.02	35.75	1.03
Girder 5	0.50	0.1046	36.0	100.0	1.00	40.56	3.29*	20.73	18.63	39.36	1.03
Girder 6	0.75	0.1046	36.0	36.0	1.00	55.14	6.08	34.93	11.18	46.11	1.20
Girder 7	1.00	0.1046	36.0	36.0	1.00	63.67	7.62	46.57	11.18	57.75	1.10
Girder 8	0.50	0.0747	36.0	36.0	1.00	28.66	5.10	19.68	5.70	25.38	1.13
Girder 9	0.50	0.1345	36.0	36.0	1.00	36.59	4.16*	20.73	18.48	39.21	0.93

*a is less than $N/2$, hence $N/2$ was used in calculatiing P_{fl}.

local bending or crippling of the web. The second, mode II, does not include a flange collapse mechanism and the failure was due to web yielding followed by crippling. The failure loads can be calculated from the following equations which were developed based on the observed failure modes. Failure modes I and II will be referred to, from hereafter, as web crippling and web yielding, respectively.

Web Crippling

The ultimate load for this mode of failure P_u consists of two components; one represents the flange capacity P_{fl} which can be determined from the flange collapse mechanism, and the second represents the web capacity P_w which can be calculated based on an empirical equation developed for girders with flat web.[26] Using the three-hinge collapse mechanism of the flange, and assuming the location of the hinges to achieve good correlation between the calculated capacity using this simple approach and the capacity calculated from the finite element analysis, the ultimate capacity of the flange can be calculated as follows

$$P_{fl} = 4M_{pf} / [a - (N/4)] \tag{5}$$

where

M_{pf} = flange plastic moment capacity = $b_f F_{yf} t_f^2 / 4$
b_f = flange width
F_{yf} = yield stress of flange material
t_f = flange thickness
N = width of patch load
a = distance between the plastic hinges at the positive and negative bending moments locations, or
$a = [(F_{yf} b_f t_f^2) / (2F_{yw} t)]^{0.5} + N/4$
$a \geq N/2$
F_{yw} = yield stress of web material
t = web thickness

The crippling capacity of the web can be calculated from the formula developed by Bergfelt[26] and assuming k_2 is equal to one, thus

$$P_w = (EF_{yw})^{0.5} t^2 \tag{6}$$

The crippling capacity can be calculated as

$$P_u = P_c = P_{fl} + P_w \tag{7}$$

The observed mode of failure for the case of loading where the patch load was over a horizontal fold was always of mode I. The calculated P_{fl} and P_w and the summation $P_u = P_c$ are given in Tables 3-1 to 3-5 for the profiles shown in Figure 4. As can be noted the correlation between the ultimate capacity ob-

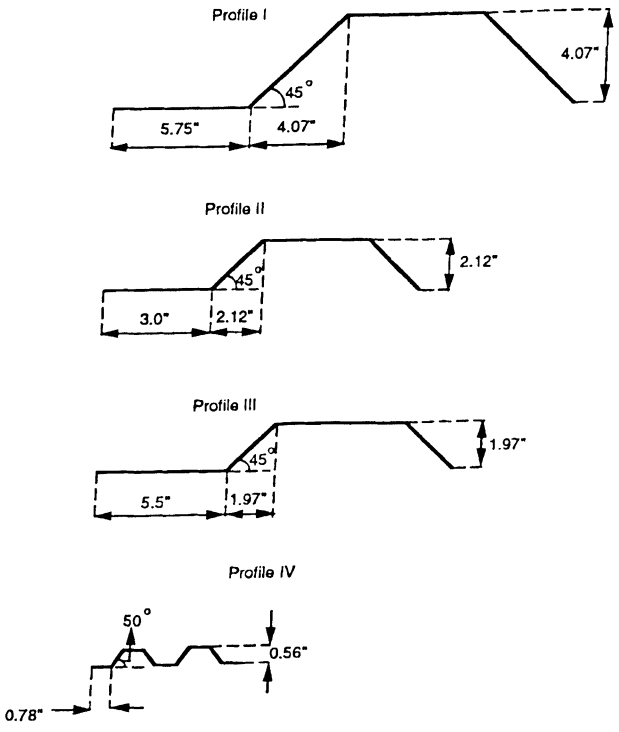

Fig. 4. Profiles considered to study effect of compressive edge loading.

Table 3-2.
Load Over a Parallel Fold, Profile I (cont.)

Girder	t_f (in.)	t_w (in.)	F_{yf} (ksi)	F_{yw} (ksi)	N/b_h	P_f (kips)	a (in.)	P_{fl} (kips)	P_w (kips)	P_u (kips)	P_f/P_u
Girder 1	0.50	0.1046	36.0	36.0	1.00	34.59	4.53*	20.73	11.18	31.91	1.08
Girder 1B	0.50	0.1046	36.0	36.0	0.33	29.50	3.57*	16.23	11.18	27.43	1.08
Girder 1C	0.50	0.1046	36.0	36.0	1.00	27.43	3.09	14.66	11.18	25.84	1.03

*a is less than $N/2$, hence $N/2$ was used in calculatiing P_{fl}.

Table 3-3.
Load Over a Parallel Fold, Profile II

Girder	t_f (in.)	t_w (in.)	F_{yf} (ksi)	F_{yw} (ksi)	N/b_h	P_f (kips)	a (in.)	P_w (kips)	P_{fl} (kips)	P_u (kips)	P_f/P_u
Girder 11	0.75	0.1345	36.0	36.0	1.00	58.06	4.29	18.48	34.30	52.78	1.10
Girder 11A	0.75	0.1345	36.0	36.0	0.67	56.17	4.04	18.48	34.30	52.78	1.06
Girder 12	0.75	0.1345	100.0	36.0	1.00	67.01	6.65	18.48	57.17	75.65	0.89
Girder 13	0.75	0.1345	36.0	65.0	1.00	85.54	3.39	24.84	46.09	70.93	1.21
Girder 14	0.75	0.1345	36.0	100.0	1.00	112.65	2.88	30.81	57.17	87.98	1.28
Girder 15	0.75	0.1046	36.0	36.0	1.00	45.12	4.77	11.18	30.25	41.43	1.09
Girder 16	0.75	0.0747	36.0	36.0	1.00	29.76	5.50	5.70	25.56	31.26	0.95
Girder 17	0.50	0.0747	36.0	100.0	1.00	43.45	2.65	9.50	28.40	37.90	1.15
Girder 17A	0.50	0.0747	36.0	100.0	0.67	39.63	2.40*	9.50	26.25	35.75	1.11
Girder 18	0.50	0.0747	36.0	65.0	1.00	38.51	3.11	7.66	22.90	30.56	1.26
Girder 19	0.50	0.0747	36.0	36.0	1.00	25.89	3.92	5.70	17.04	22.74	1.14
Girder 20	0.50	0.0747	36.0	100.0	0.00	35.50	1.90*	9.50	21.09	30.59	1.16
Girder 21	0.50	0.0747	36.0	65.0	0.00	32.63	2.36*	7.66	21.09	28.75	1.14
Girder 22	0.50	0.0747	36.0	36.0	0.00	23.67	3.17	5.70	17.04	22.74	1.04

*a is less than $N/2$, hence $N/2$ was used in calculatiing P_{fl}.

tained from the finite element analysis P_f and from the simple equations given above is very good.

Web Yielding

This mode of failure was observed for the cases of loading where the patch load was over an inclined fold or a fold line between an inclined and a horizontal fold. The ultimate capacity P_u for this mode of failure can be calculated based on yielding of an effective width of the web. The effective width was developed to give good correlation with the finite element analysis results. The ultimate capacity $P_u = P_v$ can be calculated using the following equation

$$P_u = P_v = (b + b_a)tF_{vw} \tag{8}$$

where

b = b_i or $(b_{ih} + b_h)/2$ for the load over an inclined fold or the fold line, respectively
b_i = width of the inclined fold of the profile
b_{ih} = horizontal projected length of the inclined fold of the profile
b_h = width of the horizontal fold of the profile
$b_a = \alpha t_f (F_{yf}/F_{yw})^{0.5}$
$\alpha = 14 + 3.5\beta - 37\beta^2 \geq 5.5$
$\beta = h_r/b_f$
h_r = depth of the corrugation
b_f = flange width

When the load was applied over an inclined fold or on the fold-line, the mode of failure was observed to be either mode I or II, and in some cases it was a combination thereof. It is suggested that the crippling and yield loads based on Equations 7 and 8, respectively, be calculated and the smaller of the two will control. The ultimate capacities P_u are listed in Tables 4.1 to 4.4 for cases where the load was applied over an inclined fold for different corrugation profiles and in Table 5 for cases where the load was applied over the fold-line. The smaller of the two calculated capacities is compared with the value obtained from the finite element analysis P_f, as shown in Tables 4 and 5. As can be noted, the agreement between the capacities calculated using Equations 7 and 8 and those obtained from the non-linear finite element analysis is very good.

INTERACTION BETWEEN PARTIAL COMPRESSIVE EDGE LOADING AND BENDING OR SHEAR

As in the case of flat webs, the presence of bending or shear will reduce the capacity of the girder under compressive edge loading. To study and quantify this effect, finite element analysis was performed on girders subjected to patch loading and bending or shear. Two corrugation profiles and homogeneous and hybrid girders were considered; the patch load was applied either over a horizontal or an inclined fold of the

Table 3-4.
Load Over a Parallel Fold, Profile II (cont.)

Girder	t_f (in.)	t_w (in.)	F_{yf} (ksi)	F_{yw} (ksi)	N/b_h	P_f (kips)	a (in.)	P_{fl} (kips)	P_w (kips)	P_u (kips)	P_f/P_u
Girder 23	0.4724	0.0984	69.0	48.62	0.00	41.28	5.35	38.08	11.50	49.58	0.83
Girder 24	0.4724	0.0984	69.0	46.00	0.00	36.72	4.09	37.04	11.18	48.22	0.76
Girder 25	0.4724	0.0984	69.0	46.00	1.00	41.20	5.46	37.04	11.18	48.22	0.86

Table 3-5.
Load Over a Parallel Fold, Profile IV

Girder	t_f (in.)	t_w (in.)	F_{yf} (ksi)	F_{yw} (ksi)	N/b_h	P_f (kips)	a (in.)	P_{fl} (kips)	P_w (kips)	P_u (kips)	P_f/P_u
Girder 26	0.50	0.1046	36.0	36.0	0.00	27.02	1.89	14.26	11.18	25.44	1.06
Girder 27	0.75	0.1345	36.0	100.0	0.33	74.50	1.56	40.42	30.81	71.23	1.05
Girder 28	0.50	0.1046	65.0	36.0	0.00	39.34	2.54	19.16	11.18	30.34	1.30

corrugation. The results from these analytical studies are presented in the following.

Effect of In-Plane Bending

Girders with webs made of two different profiles, and flanges of the same yield stress (36 ksi) as the web (homogeneous) or a yield stress of 65 ksi (hybrid) were considered. The thickness of the web was 0.1046-in. and the flange had a rectangular cross section which is 8-in. wide and 0.5-in. thick in the case of the girders with profile I, and the thickness of the web was 0.1345-in. and the flange was 6×0.75-in. in the case of the girders made of profile II. The patch load was applied over a horizontal or an inclined fold together with uniform bending, and the girders were analyzed using finite element models. In particular five girders were considered; a homogeneous girder with web profile I, a homogeneous girder with web profile II, and a hybrid girder with web profile II. In these three girders, the load was applied over a horizontal fold of the corrugation across the total flange width and the width of the patch was equal to the width of the fold. The remaining two girders were a homogeneous girder with web profile I and a hybrid girder with web profile II; where the patch load was applied over an inclined fold of the corrugation across the total flange width and the width of the patch was equal to the projected horizontal length of the inclined fold.

The results are plotted in Figure 5; on the same figure the following two interaction equations are plotted, namely

$$(P/P_u)^2 + (M/M_u)^2 = 1 \quad (9)$$

and

$$(P/P_u)^{1.25} + (M/M_u)^{1.25} = 1 \quad (10)$$

It has to be noted that Equation 9 is the one recommended to account for the interaction between bending and patch loading in girders with flat webs.[26] The curve given by Equation 9 represents an average for the results obtained for girders with corrugated webs when the patch load is applied over an inclined fold, however, it overestimates the capacity for the cases where the load was applied over a horizontal fold. It was noted that when girders with corrugated webs are subjected to bending, the web is not stressed except for the areas very close to the flanges. Furthermore, it was found that the horizontal folds are stressed near the flanges much higher than the inclined folds.[21] Hence, the results discussed above regarding the interaction between in-plane bending and edge compressive loading are reasonable based on previous findings. The interaction curve given by Equation 10 is conservative and represents a lower bound to the results obtained from the finite element analysis; hence it is recommended for design.

Effect Of In-Plane Shear

Girders with webs made of profile I and II, and flanges of the same yield stress (36 ksi) as the web (homogeneous) or a yield stress of 65 ksi (hybrid) were considered. The thickness of the web was 0.0747-in. and the flange had a rectangular cross section which is 8-in. wide and 0.5-in. thick in the case of the girders with profile I, and the thickness of the web was 0.1046-in. and the flange was 6×1-in. in the case of the girders made of profile II. The patch load was applied over a horizontal or an inclined fold together with uniform shear, and the girders were analyzed using finite element models. In particular five girders were considered; a homogeneous girder with web profile I, a homogeneous girder with web profile II, and a hybrid girder with web profile II. In these three girders the load was applied over a horizontal fold of the corrugation across the total flange width and the width of the patch was equal to the width of the fold. The remaining two girders were a homogeneous girder with web profile I and a hybrid girder with web profile II; and in these two girders the patch load was applied over an inclined fold of the corrugation across the total flange width and the width of the patch was equal to the projected horizontal length of the inclined fold.

Table 4-1.
Load Over an Inclined Fold, Profile I

Girder	t_f (in.)	t_w (in.)	F_{yf} (ksi)	F_{yw} (ksi)	N / b_{ih}	P_f (kips)	P_y (kips)	a (in.)	P_{fl} (kips)	P_w (kips)	P_c (kips)	P_f / P_u
Girder 31	0.50	0.1046	36.0	36.0	1.0	30.37	**33.33**	4.11	23.29	11.18	34.47	0.91
Girder 31A	0.50	0.1046	36.0	36.0	0.33	29.59	**33.33**	3.43	23.29	11.18	34.47	0.86
Girder 31B	0.50	0.1046	36.0	36.0	0.00	28.47	**33.33**	3.09	23.29	11.18	34.47	0.83
Girder 32	0.50	0.1046	65.0	36.0	1.0	32.43	**37.34**	5.17	31.29	11.18	42.47	0.87
Girder 33	0.50	0.1046	100.0	36.0	1.0	32.43	**41.11**	6.17	38.81	11.18	49.99	0.79
Girder 34	0.50	0.1046	36.0	65.0	1.0	49.88	54.77	3.31	31.29	15.02	**46.31**	1.08
Girder 35	0.50	0.1046	36.0	100.0	1.0	60.94	79.60	2.87	38.81	18.63	**57.44**	1.06
Girder 36	0.75	0.1046	36.0	36.0	1.0	45.17	**39.16**	5.66	34.93	11.18	46.11	1.15
Girder 37	1.00	0.1046	36.0	36.0	1.0	49.41	**45.00**	7.20	46.57	11.18	57.75	1.10
Girder 38	0.50	0.0747	36.0	36.0	1.0	24.12	**23.80**	4.68	19.68	5.70	25.38	1.01
Girder 39	0.50	0.1345	36.0	36.0	1.0	42.27	**42.85**	3.75	26.41	18.48	44.89	0.99

Table 4-2.
Load Over an Inclined Fold, Profile II

Girder	t_f (in.)	t_w (in.)	F_{yf} (ksi)	F_{yw} (ksi)	N / b_{ih}	h_r / b_f	P_f (kips)	P_y (kips)	a (in.)	P_{fl} (kips)	P_w (kips)	P_c (kips)	P_f / P_u
Girder 41	0.75	0.1345	36.0	36.0	1.00	0.35	56.79	53.08	4.07	34.30	18.48	**52.78**	1.08
Girder 41A	0.75	0.1345	36.0	36.0	0.00	0.35	52.81	53.08	3.54	34.30	18.48	**52.78**	1.00
Girder 41B	0.75	0.1345	36.0	36.0	1.00	0.42	52.20	**46.60**	3.76	31.31	18.48	49.79	1.12
Girder 41C	0.75	0.1345	36.0	36.0	1.00	0.60	45.21	**36.32**	3.24	26.27	18.48	44.75	1.24
Girder 41D	0.75	0.1345	36.0	36.0	1.00	0.78	41.19	**36.32**	2.91	23.10	18.48	41.57	1.13
Girder 42	0.75	0.1046	36.0	36.0	1.00	0.35	45.20	**41.29**	4.55	30.25	11.18	41.42	1.10
Girder 43	0.75	0.0747	36.0	36.0	1.00	0.35	32.63	**29.49**	5.28	25.56	5.70	31.26	1.11
Girder 44	0.75	0.1345	65.0	36.0	1.00	0.35	65.14	66.35	5.29	46.09	18.48	**64.57**	1.01
Girder 45	0.75	0.1345	100.0	36.0	1.00	0.35	74.86	78.80	6.43	57.17	18.48	**75.65**	0.99
Girder 46	0.75	0.1345	36.0	65.0	1.00	0.35	78.52	**69.30**	3.17	46.09	24.84	70.93	1.13
Girder 46A	0.75	0.1345	36.0	65.0	0.00	0.35	73.27	**69.30**	2.63	46.09	24.84	70.93	1.06
Girder 47	0.75	0.1345	36.0	100.0	1.00	0.35	101.66	104.63	2.66	57.16	30.81	**87.98**	1.16
Girder 48	0.50	0.1345	36.0	36.0	1.00	0.35	43.13	**40.24**	2.89	22.87	18.48	41.35	1.07
Girder 49	1.00	0.1345	36.0	36.0	1.00	0.35	71.27	65.95	5.25	45.73	18.48	**64.22**	1.11
Girder 49A	1.00	0.1345	36.0	36.0	0.00	0.35	65.96	65.95	4.72	45.73	18.48	**64.22**	1.03

The results are plotted in Figure 6; on the same figure the following two interaction equations are plotted, namely

$$(P / P_u)^{1.8} + (V / V_u)^{1.8} = 1 \quad (11)$$

and

$$(P / P_u)^{1.25} + (V / V_u)^{1.25} = 1 \quad (12)$$

It has to be noted that Equation 11 is the one recommended to account for the interaction between shear and patch loading in girders with flat webs, Elgaaly.[26] The curve given by Equation 11 represents an average to the results obtained from the finite element analysis, while the interaction curve given by Equation 12 is conservative and represents a lower bound to these results and is recommended for design.

SUMMARY AND CONCLUSIONS

In this paper equations were given to calculate the ultimate capacity of steel girders with trapezoidally corrugated webs subjected to bending, shear, or compressive edge loading. It was determined that there is no interaction between bending and shear. The ultimate capacity under compressive edge loading, however, will be reduced due to the presence of bending or shear, and interaction curves were given to calculate the reduced capacity.

Steel girders with corrugated webs are more economical than the conventionally stiffened girders with flat webs, and it is believed that their fatigue life is longer. Research work is currently in progress at Drexel University to study the fatigue life of steel girders with corrugated webs. This paper addresses only trapezoidal corrugations; sinusoidal corrugations have been used and the applicability of the equations given in this paper or the development of new equations need to be investigated. Furthermore, the trapezoidal configurations considered are believed to be the most efficient and the equations given are applicable to similar corrugations.

ACKNOWLEDGMENTS

The work presented in this paper is part of a study conducted under grant No. MSS-9020559 from the National Science Foundation; K. P. Chong is the program director. Support was

Table 4-3.
Load Over an Inclined Fold, Profile III

Girder	t_f (in.)	t_w (in.)	F_{yf} (ksi)	F_{yw} (ksi)	N/b_{ih}	P_f (kips)	P_y (kips)	a (in.)	P_{fl} (kips)	P_w (kips)	P_c (kips)	P_f/P_u
Girder 50	0.4724	0.0984	69.0	48.62	0.00	41.53	**48.93**	3.98	38.07	11.50	49.57	0.85
Girder 51	0.3937	0.0787	69.0	40.63	1.00	27.61	**30.60**	4.55	25.94	6.72	32.66	0.90

Table 4-4.
Load Over an Inclined Fold, Profile IV

Girder	t_f (in.)	t_w (in.)	F_{yf} (ksi)	F_{yw} (ksi)	N/b_{ih}	P_f (kips)	P_y (kips)	a (in.)	P_{fl} (kips)	P_w (kips)	P_c (kips)	P_f/P_u
Girder 52	0.50	0.1046	36.0	36.0	0.00	28.64	27.91	2.01	14.26	11.18	**25.44**	1.13

Table 5.
Load Over a Fold Line Between Horizontal and Inclined Folds

Girder	t_f (in.)	t_w (in.)	F_{yf} (ksi)	F_{yw} ksi)	$N/b_{ih}+b$ h	Profile	P_f (kips)	P_y (kips)	a (in.)	P_{fl} (kips)	P_w (kips)	P_c (kips)	P_f/P_u
Girder 61	0.5000	0.1046	36.00	36.00	0.00	I	30.02	**33.33**	3.09	23.29	11.18	34.47	0.90
Girder 62	0.5000	0.1046	36.00	65.00	0.40	I	48.72	54.79	3.28	31.28	15.02	**46.30**	1.05
Girder 63	0.5000	0.0747	36.00	36.00	0.00	II	22.05	**22.34**	3.17	17.04	5.70	22.74	0.99
Girder 64	0.7500	0.1345	36.00	36.00	0.39	II	56.47	53.08	4.05	34.30	18.48	**52.78**	1.07
Girder 64A	0.7500	0.1345	36.00	36.00	1.00	II	63.05	67.61	4.82	34.30	18.48	**52.78**	1.20
Girder 65	0.5000	0.0747	36.00	100.00	0.39	II	42.62	46.20	2.40	28.40	9.50	**37.90**	1.12
Girder 66	0.3937	0.0787	69.00	40.63	0.00	III	24.88	34.94	4.06	25.94	6.72	**32.66**	0.76
Girder 67	0.5000	0.1046	36.00	36.00	0.00	IV	27.65	27.97	1.89	14.25	11.18	**25.44**	1.09
Girder 68	0.5000	0.1046	36.00	65.00	1.00	IV	39.53	38.89	1.72	19.16	15.02	**34.18**	1.16

provided by the Structural Stability Research Council and Lincoln Electric Company. Most of the analysis was performed using the University of Illinois NCSA computing facilities. The experimental results for shear and bending were from tests conducted by Dr. Robert W. Hamilton, formerly a graduate student at the university of Maine and currently an Assistant Professor at Boise State University in Idaho.

APPENDIX I. REFERENCES

1. Arsicault, M., and Lallemand, J. P., "Joint Tracking with Self-Teaching System," *Welding Journal*, December, 1990.
2. Peterson, J. M., and Cord, M. E., "Investigation of the Buckling Strength of Corrugated Webs in Shear," *Technical Note D-424*, NASA, Washington, D.C., 1960.
3. Rothwell, A., "The Shear Stiffness of Flat Sided Corrugated Webs," *Aeronautical Quarterly*, Vol. 19, Pt.3, 1968, pp. 224–234.

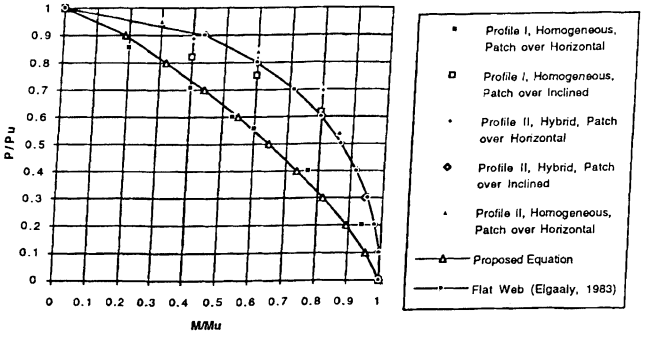

Fig. 5. Interaction between bending and compressive edge loading.

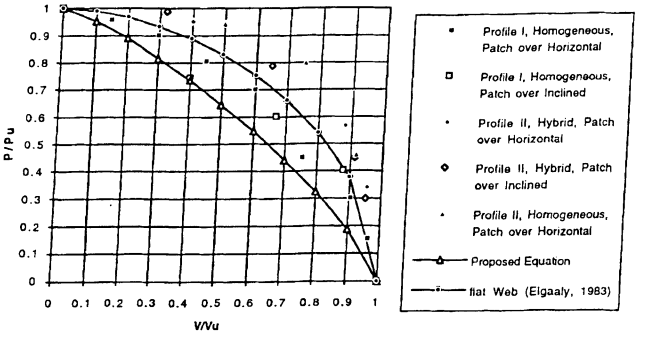

Fig. 6. Interaction between shear and compressive edge loading.

4. Sherman, D., and Fisher, J., "Beams With Corrugated Webs," *Proceedings of the First Specialty Conference on Cold-Formed Steel Structures*, University of Missouri-Rolla, 1971, pp. 198–204.
5. Libove, C., "On the Stiffness, Stress, and Buckling of Corrugated Shear Webs," *Proceedings of the Second Specialty Conference on Cold Formed Steel Structures*, University of Missouri-Rolla, 1973, pp. 259–301.
6. Libove, C., "Buckling of Corrugated Plates in Shear," *Proceedings of the International Colloquium on Structural Stability*, Structural Stability Research Council, Lehigh University, 1977, pp. 435–462.
7. Easley, J. T., "Buckling Formulas for Corrugated Metal Shear Diaphragms," *Journal of the Structural Division*, ASCE, St. 7, 1975, pp. 1403–1417.
8. Wu, L. H., and Libove C., "Curvilinearly Corrugated Plates in Shear," *Journal of the Structural Division*, ASCE, St. 11, 1975, pp. 2205–2222.
9. Hussain, M. I., and Libove, C., "Stiffness Tests of Trapezoidal Corrugated Shear Webs," *Journal of the Structural Division*, ASCE, St. 5, 1977, pp. 971–987.
10. Harrison, J. D., "Exploratory Fatigue Tests of Two Girders with Corrugated Webs," *British Welding Journal*, 12, No. 3, 1965, pp. 121–125.
11. Korashy, M., and Varga, J., "Comparative Evaluation of Fatigue Strength of Beams with Web Plate Stiffened in the Traditional Way and by Corrugation," *Acta Technica Academiae Scientiarum Hungaricae*, 1979, pp. 309–346.
12. Bergfelt, A., and Leiva-Aravena, L., "Shear Buckling of Trapezoidally Corrugated Girder Webs," *Report No. S 84:2* (ISSN 0534-0411), Department of Structural Engineering, Chalmers University of Technology, Göteborg, Sweden, 1984.
13. Lindner, J., "Lateral-Torsional Buckling of Beams with Trapezoidally Corrugated Webs," *Proceedings of the 4th International Colloquium on Stability of Steel Structures*, Budapest, Hungary, 1990.
14. Lindner, J., "Shear Capacity of Beams with Trapezoidally Corrugated Webs and Openings", *Proceedings of the Structural Stability Research Council*, Chicago, IL, 1991, pp. 403–412.
15. Scheer, J., and Einsiedler, O., "Trapezstegtrager Geschweibt Endbuicht", Bericht Nr. 6203/2, Institut fur Stahlbau Technischen, Universitat Braunschweig, Germany, 1993.
16. Hamada, M., Nakayama, K., Kakihara, M., Saloh, K., and Ohtake, F., "Development of Welded I-Beam with Corrugated Web," *The Sumitomo Search*, No. 29, 1984, pp. 75–90.
17. Heywood, P., "Corrugated Box-Girder Web Lowers Bridge Weight and Cost," *ENR*, December, 1987, 32.
18. Combault, J., "The Maupre Viaduct Near Charolles, France," *Proceedings of the AISC Engineering Conference*, 1988, 12.1–12.22.
19. Elgaaly, M., and Dagher, H., "Beams and Girders with Corrugated Webs," *Proceedings of the SSRC Annual Technical Session*, Lehigh University, 1990, pp. 37–53.
20. Elgaaly, M., Hamilton, R., and Seshadri, A., "Shear Strength of Beams with Corrugated Webs," *Journal of Structural Engineering*, ASCE, Vol. 122, No. 4, 1996.
21. Elgaaly, M., Seshadri, A., and Hamilton, R., "Bending Strength of Steel Beams with Corrugated Webs," ASCE, Accepted for publication in the *Journal of Structural Engineering*, 1997.
22. Elgaaly, M., and Seshadri, A., "Girders with Corrugated Webs Under Partial Compressive Edge Loading," ASCE, Accepted for publication in the *Journal of Structural Engineering*, 1997.
23. Hamilton, R., "Behavior of Welded Girders with Corrugated Webs," a *thesis* submitted in partial fulfillment of the requirements for the degree of doctor of philosophy in civil engineering, University of Maine, 1993.
24. Seshadri, A., "Behavior of Steel Built-Up Girders with Corrugated Webs," a *thesis* submitted in partial fulfillment of the requirements for the degree of doctor of philosophy in civil engineering, Drexel University, 1996.
25. Levia-Aravena, L., "Trapezoidally Corrugated Panels—Buckling Behavior Under Axial Compression and Shear," Division of Steel and Timber Structures, Chalmers University of Technology, Publ. 87:1, 1987.
26. Elgaaly, M., "Web Design Under Compressive Edge Loads," *Engineering Journal*, AISC, 4th Qtr., 1983, pp. 153–171.

APPENDIX II. NOTATION

The following symbols are used in this paper:

a = Distance between the plastic hinges at the positive and negative moment locations in the flange, or web panel width
b_f = Width of the flange
b_h = Width of the horizontal fold of the profile
b_i = Width of the inclined fold of the profile
b_{ih} = Width of the horizontal projection of the inclined fold of the profile
E = Young's modulus of elasticity, 29,000 ksi
F_{yf} = Yield stress of flange material
F_{yw} = Yield stress of web material
h = Web depth
h_r = Depth of corrugation
k_s = Elastic shear buckling stress coefficient
M = Moment capacity in the presence of patch loading
M_{pf} = Flange plastic moment capacity
M_u = Ultimate moment capacity in the absence of patch loading
N = Width of patch load
P = Patch loading capacity in the presence of a moment or shear

P_c = Web crippling capacity
P_e = Experimental patch loading capacity
P_f = Analytical patch loading capacity from finite element analysis
P_{fl} = Flange capacity calculated from a mechanism
P_u = Ultimate patch load capacity in the absence of a moment or shear
P_y = Web yielding capacity
t_f = Flange thickness
t = Web thickness
V = Shear capacity in the presence of patch loading
V_u = Ultimate shear capacity in the absence of patch loading
w = Fold width
α = Empirical coefficient
μ = Poisson's ratio
θ = Angle of inclination of an inclined fold
τ_{cre} = Elastic shear buckling stress
τ_{cri} = Inelastic shear buckling stress
τ_y = Shear yield stress